

Cytotoxic Effects of Theranekron D6 on HepG2 Hepatocellular Carcinoma Cells

Deniz Şumnu 1,a,*

¹ Technology Research Development Application and Research Center, Trakya University, Edirne, Türkiye.

*Corresponding author

Research Article

History

Received: 20/09/2023

Accepted: 25/02/2024



This article is licensed under a Creative Commons Attribution-NonCommercial 4.0 International License (CC BY-NC 4.0)

ABSTRACT

Theranekron D6 is an alcoholic extract of *Tarantula cubensis*. In this study, the cytotoxic effects of Theranekron D6 on HepG2 and on AML12 cells were investigated by MTT analyses. Gene expression analyses were performed by qRT-PCR. Apoptotic, necrotic, and healthy cells were viewed by a fluorescent microscope, and they were counted by a flow cytometry device. 143 µg/mL Theranekron D6 was calculated as an IC₅₀ value for HepG2 cells, and it was applied to both cell lines. No significant increase in the amount of apoptotic and necrotic cells was observed at the AML12 cells, while both of them increased by 31.04% at the HepG2 cells by Theranekron D6 application. The accuracy of flow cytometry data was confirmed through fluorescence microscope analyses. At the HepG2 cells, significant increases were observed at the expression levels of Bax (5.61 ± 0.34), Cas3 (2.74 ± 0.34), APAF1 (3.64 ± 0.44), and p53 (2.10 ± 0.3) genes, but at the AML12 cells, the expression levels of the same genes 1.14 ± 0.14, 0.54 ± 0.17, 0.71 ± 0.17, and 0.93 ± 0.3 not increased. Based on these data, it was concluded that Theranekron D6 may be a chemotherapy candidate for HepG2 cells.

Keywords: AML12, Anticancer, Cytotoxicity, HepG2, *Tarantula cubensis* D6.✉ denizsumnu@trakya.edu.trORCID <https://orcid.org/0009-0009-0693-3569>

Introduction

Hepatocellular carcinoma (HCC) has an incidence of 90% among all types of liver cancer and ranks first in terms of death among all cancer types [1, 2]. HCC ranks 5th among all cancer types in men and 9th in women and is the second deadliest type of cancer worldwide [3]. In the triggering of HCC, cirrhosis due to chronic liver damage caused by fibrosis, hepatitis B (HBV) and hepatitis C (HCV) virus infection, alcohol addiction, and metabolic syndrome are stated to be risk factors [4]. Apart from these, the consumption of tobacco products and the intake of aflatoxin B1 (a cancer-triggering fungus found in foods) have also been primarily associated with HCC [2, 5]. More than 850,000 individuals are diagnosed with HCC each year [2].

The fact that the diagnosis of HCC is usually made once the cancer has reached advanced stages limits the possible methods of treatment. Because of this, the life expectancy of patients with HCC is usually between six and twenty months once they are diagnosed. According to studies conducted on American individuals, there is less than a 50% chance of a two-year and less than a 10% chance of a five-year life expectancy after diagnosis for all HCC cases [6, 7]. In the fight against advanced HCC, chemotherapeutic drugs such as sorafenib, regorafenib, and lenvatinib are frequently used to prolong the quality and duration of life in patients [8].

For many years, scientists have been researching the possible benefits of the venoms of various living species to treat many types of cancer. Especially in ancient Greek, Indian, and Chinese medicine, many kinds of animal

venoms are frequently used in the fight against various cancer types [9]. According to some studies on breast cancer, the venoms of the Chinese Red Scorpion (*Buthus martensi*), the Yellow Persian Scorpion (*Odontobuthus doriae*), the Arabian Thicktail Scorpion (*Androctonus crassicauda*), the Chinese Scorpion (*Buthus matensii Karsch*), Venezuelan Scorpion (*Tityus discrepans*) have been reported to induce apoptosis of MDA 435, MCF-7, and SKBR3 cell lines [10-14]. In addition, the apoptotic effects of Brazilian Yellow Scorpion (*Tityus serrulatus*) venom on SiHa and HeLa cervical adenocarcinoma cell lines have been demonstrated [15].

Although snake venom has positive effects on cancer, it has been revealed that the antineoplastic effects of scorpion venom are much more promising than snake venom [16, 17]. Similar to these studies, in this study the apoptotic effects of Theranekron D6 (TD6) on HepG2 cell lines were investigated. TD6 is an alcoholic extract of *Tarantula cubensis* D6. Although it has long been known that TD6 has anti-inflammatory, demarcative, necrotizing, and resorptive effects and has been used in wound healing [18], the main purpose of its application in animal health is to treat oral, skin, and nipple papillomatosis [19-21]. It is also used to treat animal diseases such as panaritium, laminitis, foot rot, and arthritis [22]. Recently, the anticancer activity of TD6 has been reported in canine mammary tumors [23].

Apoptosis is the controlled cell death mechanism used to fight many cancer types. Reactive oxygen species (ROS) cause upregulation of apoptosis via mitochondrial apoptotic pathway genes. Some studies showed that snake venom toxins enhance ROS in mitochondria and cause inhibition of cancer cell growth by mitochondrial apoptotic signaling pathway genes [24-26]. The apoptotic effect of TD6 in HCC cells has not been thoroughly investigated. The present study describes the mitochondrial apoptotic effect of TD6 in the HepG2 cell line via oxidative stress mechanisms.

Materials and Methods

Cell Culture

Human hepatocellular carcinoma (HepG2) (ATCC, USA) and human healthy liver cell line (AML12) (ATCC) were maintained in "Dulbecco's Modified Eagle's Medium/Nutrient F-12 Raw", 10% fetal bovine serum (SIGMA-ALDRICH, USA), 2 mM L-Glutamine (Thermo-Fisher, USA), and 100 IU/ml penicillin-streptomycin (Thermo-Fisher). Theranekron D6 was purchased from Richter Pharma (Germany). Cells were cultured in a humidified incubator at 37°C and 5% carbon dioxide.

3-(4,5-dimethylthiazol-2-yl)-2,5-diphenyl tetrazolium bromide (MTT) analyzes

AML12 and HepG2 cell lines were separately seeded in 180 µl volumes with approximately 5×10^3 cells in each well on 96-well spectrophotometric plates (NEST, USA). Cells were treated with 8.9, 17.8, 35.75, 71.5, 143, 286 µg/mL concentrations of TD6 for 24 h. After treatments, 20 µl of MTT (5 mg/ml) solution was applied to each well, and plates were incubated at 37°C for 3 h in 95% humidity and 5% CO₂. At the end of the incubation, all the liquid phase on the cells was removed, and 180 µl dimethyl sulfoxide (DMSO) was applied for 20 min to each well. The viability of the cells was calculated by reading the absorbance value at 570 nm wavelength in the Thermo Scientific Multiskan GO spectrophotometer device (USA).

Cell Fluorescent Staining

AML12 and HepG2 cells were separately seeded in 4 wells of 6-well plates (NEST) with 5×10^4 cells per well. No substance was applied to two wells, and they were used as AML12 and HepG2 controls. 143 µg/mL TD6 was applied to the other two wells of both cell lines for 24 h. At the end of 24 h, each cell line was stained with both Annexin V-FITC/PI Apoptosis Kit (Elabscience, USA) and Hoechst 34580 (Cayman Chemical, USA) fluorescent dyes,

and microscope images were taken. For the Annexin V/PI application, at the end of 24 h, the medium on the cells was removed and washed with 1× PBS. In 2 ml 1× Annexin V binding buffer, 5 µl of Annexin V-FITC and 5 µL of PI were mixed and applied to each well for 20 min at room temperature in the dark. Images were taken on a 5× objective using the FITC channel of the Zeiss Observer Z1 fluorescent microscope. For the application of Hoechst 34580, 25 µg of Hoechst 34580 was dissolved in 50 ml of 1× PBS. After removing the medium from the cells, 2 ml of Hoechst 34580 solution was applied to each well in the dark at room temperature for 20 min. At the end of the application, cells were visualized using a 5× objective and the DAPI channel.

Flow Cytometry-Based Quantitative Apoptosis Analyses

AML12 and HepG2 cells were separately seeded into two 6-well plates, with 5×10^4 cells in each well. After 24 h of cells adhering to the plate, 3 wells of AML12 cells and 3 wells of HepG2 cells were treated with 143 µg/mL TD6 for 24 h. Other cells in both three wells were used as AML12 and HepG2 control cells. At the end of 24 h, cells in all wells were trypsinized and removed into 1.5 ml collection tubes (Eppendorf, Germany). All tubes were centrifuged in a centrifuge device (Hermle, Germany) at 300 g for 5 minutes to remove trypsin from the cells. At the end of 5 minutes, the supernatants were removed from the pellet, and the cells were resuspended in 500 µl 1× PBS. 200 µl 1× Annexin V binding buffer, 2.5 µl Annexin V-FITC, and 2.5 µl PI were mixed with the 500 µl 1× PBS and cell mixture for each sample and incubated in the dark at room temperature for 15 min. Annexin V-stained cells were counted for the BL1-A channel, PI-stained cells were counted for the BL2-A channel, and both Annexin V and PI-stained cells were counted for the BL1-A and BL2-A channels together in an Applied Biosystems Attune acoustic focusing cytometer flow cytometry device (Applied Biosystems, USA).

Total RNA Isolation, cDNA Synthesis, and RT-PCR Analyses

Total RNAs were extracted from cells using the Column Pure RNA Miniprep Kit (ABM, USA), and the OneScript Plus cDNA Synthesis Kit (ABM) was used for cDNA synthesis according to the manufacturer's protocols. RT-qPCR was performed using BlasTaq 2× qPCR MasterMix (ABM). RT-qPCR analysis is applied to the QuantStudio 6 Flex (Applied Biosystems) RT-PCR device. The primer sequences of the genes and RT-qPCR conditions are shown in Table 1.

Table 1. Gene codes with GenBank ID, primer base sequences of genes, and RT-PCR conditions.

Gene Codes and GenBank ID	Primer Base Sequences	Real Time PCR Conditions	
Gapdh	F: CAATGCCTCCTGCACCACCA R: GATGTTCTGGAGAGCCCGC	Hold Stage: 1 Cycle 50°C 2 minute 95°C 10 minute	
NM_002046	F: GTCACCATACATGGAATGGCA R: CTGATCCAACCGTGTGCAAA		
APAF-1	F: TCCCCCTCAGATGATCTCTCCA R: CGGAAAGGTTAAGCGTCGAAAA		
NM_001160	F: GGAGGATTGTGGCCTTCTTT R: GCCCAATACGACCAATCCGTTGA		
Akt	F: CCCGAGAGGTCTTTTCCGAG R: CCAGCCCATGATGGTTCTGAT		
NM_005163	F: TGGTAACTGGTCTTAAACCGGAATC R: GGCGGTGAGTGCAGGATAGG		
BCL-2	F: GGAAGCGAATCAATGGACTCTGG R: GCATCGACATCTGTACCAGACC		PCR Stage: 40 Cycle 95°C 15 second 60°C 1 minute
NM_000657.2	F: ACCTGAAAGTTACATCCACAGAA R: GGGTGTATCCAAAACCCGGA		
Bax	F: TCTACACCCGACAACTCCATCCG R: TCTGGCATTGAGAGGAAGTG		
NM_138761	F: TCACTGTGGCTGTACCAAGGTG R: CCAGGAAGTAAAAGCATTCCAGC		
CAT	F: GGGCATGACTAATCCCCTACTGA R: GCCCAATCCTAGACGGCAAC		
NM_001752.3	F: CCTCTGACGTCCATCATCTC R: ATCTTCTGCTGCCGTCGCTT	Melt Curve Stage: 1 Cycle 95°C 15 second 60°C 1 minute 95°C 15 second	
Cas3	F: CCTGGAACCTCACATCAACG R: CCAACGCCTCCTGGTACTTC		
NM_004346	F: AGATGGACTTCAACCTGCTAGTG R: GTCAAAGAGACGAGCGGTAAG		
CD133	F: GAGATGGCAGGATCCTGTGAGC R: ATTCTGGAATTCGTCTACGATGATGACC		
NM_006017.2	F: TTGTCTGCACACTTCTGTAGTT R: AACAGTCCCATTGGATTCAACA		
CycD1	F: TATGTGAGCCGCTGAATGCCA R: CACTGACCTCTATTGTGGGCTTG		
NM_053056	F: GAGGTTGGCTCTGACTGTACC R: TCCGTCAGTAGATTACCAC		
CuZn-SOD	F: GCTACTGCCATCCAATCGAG R: TGGTGATGTTGGACTCCTCA		
NM_000454.4			
EGF			
NM_001945.3			
ErbB2			
NM_001005862.2			
Mn-SOD			
NM_001322819.2			
GS			
NM_000178.2			
GSR			
NM_000637.5			
PI3K			
NM_006218.2			
GSR			
NM_000637.5			
p53			
NM_001126118			
VEGF			
NM_001033756			

Statistical Analyses

In MTT analyses, cells without substance were considered 100% viable. The percentage of cell viability was calculated using the following formula:

Cell viability = (absorbance value of the TD6 applied wells / absorbance value of the control wells) × 100.

Three consecutive TD6 applications were calculated with the 2^{-ΔΔCT} formula. The relative gene expression levels were normalized to the glyceraldehyde 3-phosphate dehydrogenase (GAPDH) gene. Statistical significance was assessed for both RT-PCR and flow cytometry analyses using the SPSS Paired-Samples T test. P < 0.05 values were considered statistically significant.

Results

3-(4, 5-dimethylthiazol-2-yl)-2, 5-diphenyl tetrazolium bromide (MTT) Analyses

In the AML12 cell line, 98.54% and 80.96% viabilities were determined for the lowest (8.9 µg/mL) and highest (286 µg/mL) doses of TD6 application, respectively. Contrary to the AML12 cell line, 86.25%, 49.93%, and

45.92% viabilities were determined for the lowest (8.9 µg/mL), IC₅₀ (143 µg/mL), and highest (286 µg/mL) doses of TD6 application in HepG2 cells, respectively. For a 143 µg/mL TD6 application, 89.41% viability was determined in AML12 cells. TD6 exhibited selective toxicity in AML12 and HepG2 cells, and 143 µg/mL TD6 was chosen as an application dose for both cell lines (Figure 1).

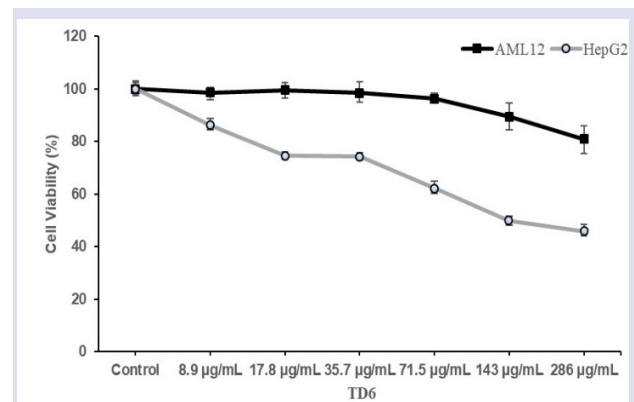


Figure 1. MTT cell viability (%) assay on the control and TD6-treated AML12 and HepG2 cells for 24 h (mean ± SD).

Gene Expression Analyses

In the AML12 cell line, statistically significant increases at gene expression levels of PI3K, Akt, EGF, VEGF (angiogenesis pathway genes), CD133 oncogene, and CycD1 cell cycle/proliferation gene were determined. Conversely, decreases were observed in the Cas3 gene expression level, and no significant changes were determined at the gene expression levels of BCL-2, Bax, APAF-1, p53 (mitochondrial apoptotic pathway genes), Mn-SOD, and GS (mitochondrial oxidative stress regulator genes). Contrary to the AML12 cell line, the expression level of CycD1 decreased, while BCL-2, Bax, APAF-1, Cas3, p53, Mn-SOD, and GS, significantly increased in the HepG2 cell line. PI3K, Akt, EGF, VEGF, and ErbB2 gene expression levels remained stable due to the TD6 application in the HepG2 cell line ($p < 0.05$) (Table 2).

Table 2. mRNA expression level changes of angiogenesis, cell cycle, apoptotic, oxidative stress, and oncogenes in AML12 and HepG2 cells due to the TD6 application (mean \pm SD) (relative to the control group; $p < 0.05$).

Genes	AML12		HepG2	
	Relative Fold Changes	P Values	Relative Fold Changes	P Values
PI3K	2.34 \pm 0.18	0.006	0.65 \pm 0.07	0.012
ErbB2	1.65 \pm 0.28	0.059	0.79 \pm 0.03	0.006
Akt	2.17 \pm 0.14	0.005	0.80 \pm 0.06	0.027
VEGF	2.35 \pm 0.28	0.022	0.78 \pm 0.16	0.128
EGF	2.76 \pm 0.29	0.009	0.75 \pm 0.21	0.162
CD133	2.85 \pm 0.11	0.001	1.07 \pm 0.25	0.765
CycD1	2.11 \pm 0.15	0.007	0.26 \pm 0.18	0.018
BCL2	0.92 \pm 0.13	0.356	4.17 \pm 0.17	0.001
Bax	1.14 \pm 0.14	0.248	5.61 \pm 0.34	0.002
Cas3	0.54 \pm 0.17	0.042	2.74 \pm 0.34	0.013
APAF1	0.71 \pm 0.17	0.094	3.64 \pm 0.44	0.009
p53	0.93 \pm 0.3	0.668	2.10 \pm 0.3	0.024
Mn-SOD	0.83 \pm 0.19	0.242	3.71 \pm 0.14	0.001
GS	0.79 \pm 0.2	0.204	6.72 \pm 0.16	0.000

Flow Cytometry-Based Quantitative Apoptosis Analyses

In the AML12 cell line, no statistically significant change in apoptotic cell quantity was observed between the control (1.84% \pm 0.97) and TD6-treated (1.23% \pm 0.41) cells. In the HepG2 cell line, the levels of early apoptosis significantly increased in the TD6-treated group (25.34% \pm 2.79) compared with the control group (3.65% \pm 2.95). Also, late apoptosis was assessed. The levels of late apoptosis were significantly higher in the TD6-applied group (9.96% \pm 5.11) compared with the control group (0.61% \pm 0.54) (Fig. 2A). The average of three repeats of the control total apoptotic cells was calculated as 4.26% \pm 2.01, while the TD6-treated apoptotic HepG2 cells were 35.3% \pm 2.52. This difference (31.04%) between the control and TD6-treated HepG2 cells was assessed as statistically significant ($p = 0.001$) (Figure 2).

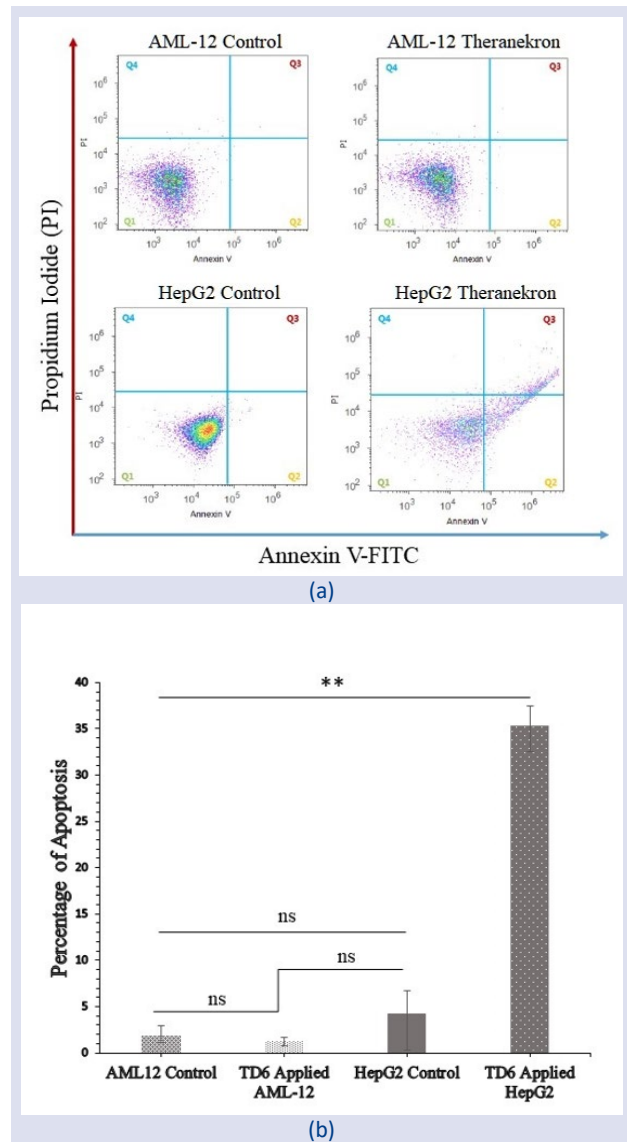


Figure 2. (a) Lower-left quadrant: viable cells unlabeled by Annexin V and PI; lower-right quadrant: early-apoptotic cells labeled by Annexin V only; upper-left quadrant: early-necrotic cells labeled by PI only; upper-right quadrant: late-apoptotic/necrotic cells labeled by both Annexin V and PI. The data are representative of three independent measurements. (b) Apoptotic rates of control and TD6-treated AML12 and HepG2 cells using Annexin V and PI double staining (mean \pm SD.) (relative to the control group; SPSS Paired-Samples T test applied; ^{ns} $p > 0.05$, * $p < 0.05$, ** $p < 0.01$).

Fluorescent Staining

In the TD6-treated HepG2 cell line, the interior of some cell membranes is stained with Annexin V (bright green), which is a marker of early apoptosis, and the nuclei of many cells are stained with PI (red), which is a marker of late apoptosis. In addition, degraded nuclei have been seen that are stained with Hoechst 34580 in the TD6-applied HepG2 cell line. Contrary to these findings, neither early nor late apoptosis markers were observed in the TD6-treated AML12 cell line (Figure 3).

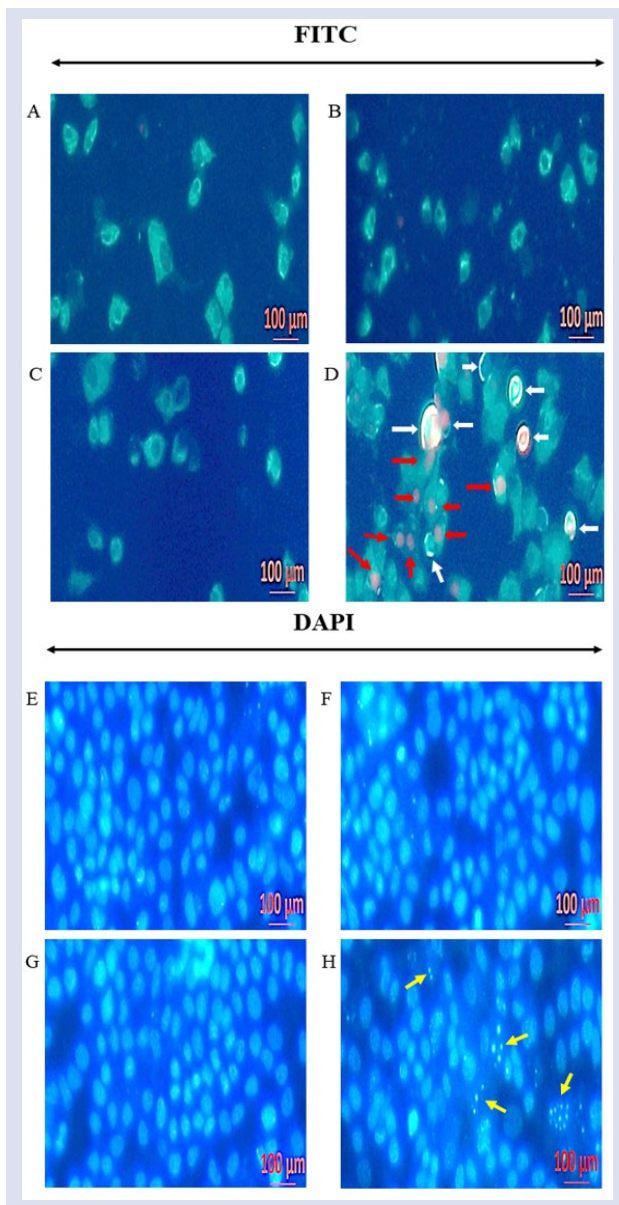


Figure 3. Fluorescence staining images of (A) and (E) control, (B) and (F) TD6-treated AML12, and (C) and (G) control, (D) and (H) TD6-treated HepG2 cells (white arrows: Annexin V-labeled early apoptotic cells; red arrows: PI-labeled late apoptotic cells; and yellow arrows: Hoechst 34580-stained nuclei degraded cells).

Discussion

In the present study, the oxidative, cytotoxic, and apoptotic effects of TD6 on the HCC HepG2 cell line and the healthy liver cell line AML12 have been investigated. Mitochondrial oxidative stress has an important role in activating the mitochondrial apoptotic pathway. Especially enhancing Mn-SOD and GS in mitochondria causes apoptosis through the mitochondrial apoptotic cascade [27]. In line with this strategy, many chemotherapy agents are being used in the fight against cancer. In a study about the induction of oxidative stress by anticancer drugs, it has been shown that doxorubicin, actinomycin D, mitomycin C, mercaptopurine, carmofur,

vinorelbine, vinblastine, camptotecin, and paclitaxel have oxidant activities that trigger apoptosis in DLD-1 human colorectal cancer cells [28]. However, some of these chemotherapeutic agents also have cytotoxic effects on healthy cells and tissues. Therefore, in this study, the cytotoxic effect of TD6 was investigated by applying 8.9-286 µg/mL doses to both the carcinoma cell line HepG2 and the healthy cell line AML12 for 24 h. It was determined from MTT analysis that the highest dose of 286 µg/mL suppressed only 19.04% cell proliferation in the AML12 cell line, whereas 143 µg/mL suppressed 50.07% cell proliferation in the HepG2 cell line. In a study, the human embryonic kidney cell line (HEK-293), human breast cancer cell line (MCF-7), human small cell lung cancer cell line with multidrug-resistant variant (H69AR), and human prostate cancer cell line (PC3), the most appropriate IC_{50} values of TD6 were investigated depending on the application doses range of 10-100 µg/mL for 24, 48, and 72 hours. In this study, IC_{50} values based on 72 hours of application time for HEK-293, MC-7, H69AR, and PC3 cell lines were calculated as 88.3 µg/mL, 94.7 µg/mL, 295 µg/mL, and 118.9 µg/mL. Remarkably, in this study, the IC_{50} value for the healthy HEK-293 cell line is lower than the IC_{50} value determined for cancerous cell lines, which shows that, TD6 has a more cytotoxic effect on the healthy cell line than on cancerous cell lines [29]. In another study, prostate (PC3), breast (MDA-MB-231), lung (H69), and ovarian (OVCAR-3) cancer cell lines and a non-cancerous epithelial (MCF-10A) cell line were treated with another *Tarantula cubensis* product called "Tarantula-Logoplex" (Richter Pharma) with a dose range of 10-500 µg/mL for 24, 48, and 72 hours, and the IC_{50} values were investigated. In this study, IC_{50} values for the cell lines in the order specified, depending on the 72-hour application time of Tarantula-Logoplex (TL), were calculated as 40.2 ± 1.2 , 159.3 ± 2.1 , 498.3 ± 1.2 , 48.9 ± 1.8 , and 217.8 ± 2.0 µg/mL [30]. From this study, the IC_{50} value determined for the healthy epithelial cell line (MCF-10A) is higher than those determined for prostate (PC3), breast (MDA-MB-231), and uterine (OVCAR-3) cancer cell lines, showing that the cytotoxic effect of TL is higher for these three cancerous cell lines than for the healthy epithelial cell line. However, the IC_{50} value for the lung cancer (H69) cell line is more than twice the IC_{50} value of the healthy epithelial cell line, indicating that TL has a more cytotoxic effect on MCF-10A than H69. As seen from these studies, the acholic extract of *Tarantula cubensis* has a selective cytotoxic effect on different cancer cell lines. According to the MTT analysis performed in the present study, depending on the application dose of 8.9-286 µg/mL TD6 to the healthy liver cell line (AML12) and hepatocellular carcinoma cell line (HepG2), the proliferation was suppressed by 50.07% in the HepG2 cell line for 143 µg/mL TD6, while in the AML12 cell line only 10.59% of suppression was observed by the same dose of TD6. In order to investigate this selective effect of TD6 on cytotoxicity, 143 µg/mL of TD6 (the IC_{50} value of the cancerous cell line HepG2) was chosen as the reference application dose for both cell lines.

RT-PCR analysis showed that 143 µg/mL of TD6 promoted mitochondrial apoptosis by increasing mitochondrial oxidative stress in HepG2 cells via significant increases in expression levels of Mn-SOD, GS, BCL-2, Bax, Apaf-1, Cas3, and p53 genes ($p < 0.05$). Mitochondria are the source of cellular ROS. Excessive production of ROS causes oxidative stress, and if oxidative stress is not normalized in the mitochondria by scavenger enzyme genes (Mn-SOD and GS), the mitochondrial apoptotic pathway induces apoptosis [31]. The enhancement of BCL-2, Bax, APAF-1, Cas3, and p53 gene expression levels indicates that oxidative stress genes were not able to scavenge ROS in HepG2 cells. In addition, a significant decrease in the expression level of the CycD1 gene indicates that the HepG2 cell line could not pass the G0/ G1 phase in the cell cycle, and HepG2 cells went into apoptosis. Contrary to HepG2 cells, it was determined that TD6 has not stimulated apoptosis due to the significant increase in the expression levels of CycD1 and PI3K/ Akt/ EGF/ VEGF angiogenesis pathway genes in the AML12 cell line ($p < 0.05$) and also that oxidative stress gene expression levels remain stable.

The other important apoptosis indicators are Annexin V and PI stains. Annexin V exerts high affinity to phosphatidyl serine (PS) residues via Ca^{2+} cations. PS are translocated to the inner membrane of the cells, both in the apoptotic and necrotic stages, but initial of the apoptosis the cell membrane remains intact, while late stage of apoptosis and necrosis the cell membrane loses its integrity and becomes leaky. Annexin V is a little molecule, so at the initiation of apoptosis, only Annexin V passes through into the cell membrane, but at the late stage of apoptosis and necrosis, PI, which is the bigger molecule than Annexin V, passes through the membrane and reaches the nuclei of the cell and binds to it. Under the fluorescent microscope using both the FITC and PI channels, the early stage of apoptotic cells is seen as bright green due to the FITC channel, but at the late stage of apoptosis and necrosis, the cell nuclei are seen as red due to the PI channel of the fluorescent microscope [32]. In this study, both early and late apoptosis were demonstrated in TD6-applied HepG2 cells via Annexin V and PI staining methods in the fluorescence microscope, but there was no apoptotic sign in the AML12 cell line by the same application. Moreover, flow cytometry analysis provided numerical support for demonstrating these apoptotic events. Hoechst 34580 and its derivatives (Hoechst 33258 and Hoechst 33342) have a high affinity for DNA, and they are frequently used in anti-cancer drug studies to view both the nuclei of live and apoptotic or necrotic cells [33]. In this study, the result of the Hoechst 34580 staining assay showed that some nuclei degraded cells in the HepG2 cell line, but no apoptotic sign was detected by the same application in the AML12 cell line.

Conclusion

TD6 causes apoptosis via enhanced reactive oxidative species and trigger to mitochondrial apoptotic pathway in

the HepG2 cell line. However, there is less cytotoxic effect in the healthy AML12 cell line. This selective feature indicates the importance of Theranekron D6 in cancer studies. However, further in vitro and in vivo researches are needed to use TD6 in HCC and other types of cancer treatments, and more effective results can be obtained by combining it with currently used cancer drugs.

Conflicts of interest

There are no conflicts of interest in this work.

Acknowledgement

Thanks for all laboratory equipment supplied by Trakya University Technology Research Development Application and Research Center (TUTAGEM) and Apothecary Zeynep Meral Şahin, who was suggested to Theranekron D6 in cancer application.

References

- [1] Ferlay J., Soerjomataram I., Dikshit R., Eser S., Mathers C., Rebelo M., Parkin D.M., Forman D., Bray F., Cancer incidence and mortality worldwide: sources, methods and major patterns in GLOBOCAN 2012, *Int J Cancer*, 136(5) (2015) E359–86.
- [2] Torre L., Global cancer statistics, 2012, *CA-CANCER J CLIN*, 65(2) (2015) 87–108.
- [3] Park J.W., Chen M., Colombo M., Global patterns of hepatocellular carcinoma management from diagnosis to death: the BRIDGE Study, *LIVER INT*, 35(9) (2015) 2155–2166.
- [4] EASL-EORTC clinical practice guidelines: management of hepatocellular carcinoma, *J Hepatol.*, 56(4) (2012) 908–43.
- [5] Laursen L., A preventable cancer, *Nature*, 516(7529) (2014) S2–3.
- [6] McGlynn KA, London W.T., “The global epidemiology of hepatocellular carcinoma: present and future”, *Clin Liver Dis.*, 15(2) (2011) 223–x.
- [7] McGlynn K.A., Petrick J.L., London W.T., “Global epidemiology of hepatocellular carcinoma: an emphasis on demographic and regional variability”, *Clin Liver Dis.*, 19(2) (2015) 223–38.
- [8] Sim H.W., Knox J., Hepatocellular carcinoma in the era of immunotherapy, *Curr Probl Cancer*, 42(1) (2018) 40–48.
- [9] Gomes A., Bhattacharjee P., Mishra R., Biswas A.K., Dasgupta S.C., Giri B., Anticancer potential of animal venoms and toxins, *Indian J Exp Biol.*, 48(2) (2010) 93-103.
- [10] Chang N.S., Transforming growth factor-beta protection of cancer cells against tumor necrosis factor cytotoxicity is counteracted by hyaluronidase (review), *Int J Mol Med*, 2(6) (1998) 653-9.
- [11] Zargan J., Sajad M., Umar S., Naime M., Ali S., Khan H.A., Scorpion (*Odontobuthus doriae*) venom induces apoptosis and inhibits DNA synthesis in human neuroblastoma cells, *Mol Cell Biochem.*, 348(1-2) (2011) 173-81.
- [12] Caliskan F., Garcia B.I., Coronas F.I., Batista C.V., Zamudio F.Z., Possani L.D., Characterization of venom components

- from the scorpion *Androctonus crassicauda* of Turkey: peptides and genes, *Toxicon*, 48(1) (2006) 12-22.
- [13] D'Suze G., Rosales A., Salazar V., Sevcik C., Apoptogenic peptides from *Tityus discrepans* scorpion venom acting against the SKBR3 breast cancer cell line, *Toxicon*, 56(8) (2010) 1497-505.
- [14] Li H.M., Wang D.C., Zeng Z.H., Jin L., Hu R.Q., Crystal structure of an acidic neurotoxin from scorpion *Buthus martensii* Karsch at 1.85 Å resolution, *J Mol Biol.*, 261(3) (1996) 415-31.
- [15] Oliveira E.B., Farias K.J.S., Gomes D.L., de Araújo J.M.G., da Silva W.D., Rocha H.A.O., Donadi E.A., Fernandes-Pedrosa M.F., Crispim J.C.O., *Tityus serrulatus* Scorpion Venom Induces Apoptosis in Cervical Cancer Cell Lines. Evid Based Complement Alternat Med., 2019: 5131042.
- [16] Fu Y.J., Yin L.T., Liang A.H., Zhang C.F., Wang W., Chai B.F., Fan X.J., Therapeutic potential of chlorotoxin-like neurotoxin from the Chinese scorpion for humangiomas, *Neurosci Lett.*, 412(1) (2007) 62-7.
- [17] Mamelak A.N., Jacoby D.B., Targeted Delivery of Antitumoral Therapy to Glioma and Other Malignancies with Synthetic Chlorotoxin (TM-601), *Expert Opin Drug Deliv.*, 4(2) (2007) 175-86.
- [18] Stampa S., A field trial comparing the efficacy of sulphamonomethoxine, penicillin, and tarantula poison in the treatment of pododermatitis circumspecta of cattle, *J S Afr Vet Assoc.*, 57(2) (1986) 91-3.
- [19] Cam Y., Kibar M., Atasever A., Atalay O., Beyaz L., Efficacy of levamisole and *Tarantula cubensis* venom for the treatment of bovine cutaneous papillomatosis, *Vet Rec.*, 160(14) (2007) 486-8.
- [20] Icen H., Sekin S., Simsek A., Kochan A., Tunik S., The efficacy of *Tarantula cubensis* extract (Theranekron) in treatment of canine oral papillomatosis, *Asian J Anim Vet Adv.*, 6(7) (2011) 744-749.
- [21] Paksoy Z., Gülesci N., Kandemir F.M., Dinçel G.Ç., Effectiveness of levamisole and tarantula *cubensis* extract in the treatment of teat Papillomatosis of cows, *Indian J Anim Res.*, 49(5) (2015) 704-8.
- [22] Sardari K., Kakhki E.G., Mohri M., Evaluation of wound contraction and epithelialization after subcutaneous administration of TheranekronR in cows, *Comp Clin Path.*, 16(3) (2007) 197-200.
- [23] Gultiken N., Guvenc T., Kaya D., Agaoglu A.R., Ay S.S., Kucukaslan I., Emre B., Findik M., Schafer-Somi S., Aslan S., *Tarantula cubensis* extract alters the degree of apoptosis and mitosis in canine mammary adenocarcinomas, *J Vet Sci.*, 16(2) (2015) 213-9.
- [24] Al-Asmari A.K., Riyasdeen A., Al-Shahrani M.H., Islam M., Snake venom causes apoptosis by increasing the reactive oxygen species in colorectal and breast cancer cell lines, *Onco Targets Ther.*, 15 (2022) 1289.
- [25] Akhtar B., Muhammad F., Sharif A., Anwar M.I., Mechanistic insights of snake venom disintegrins in cancer treatment, *Eur J Pharmacol.*, 899 (2021) 174022.
- [26] Chong H.P., Tan K.Y., Tan C.H., Cytotoxicity of snake venoms and cytotoxins from two southeast Asian cobras (*Naja sumatrana*, *Naja kaouthia*): exploration of anticancer potential, selectivity, and cell death mechanism, *Front Mol Biosci.*, 7 (2020) 583587.
- [27] Orrenius S., Gogvadze V., Zhivotovsky B., Mitochondrial Oxidative Stress: Implications for Cell Death, *Annu Rev Pharmacol Toxicol.*, 47 (2007) 143-183.
- [28] Yokoyama C., Sueyoshi Y., Ema M., Mori Y., Takaishi K., Hisatomi H., Induction of oxidative stress by anticancer drugs in the presence and absence of cells, *Oncol Lett.*, 14(5) (2017) 6066-70.
- [29] Çamlı Pulat Ç., In vitro cytotoxic activity of *Tarantula cubensis* alcoholic extract on different human cell lines. *Cumhuriyet Sci. J.*, 42(2) (2021) 252-259.
- [30] İlhan S., Can a Veterinary Drug be Repurposed for Human Cancers?: Cytotoxic Effect of *Tarantula cubensis* Venom on Human Cancer Cells. *Journal of the Institute of Science and Technology*, 11(3) (2021) 1763-1769.
- [31] Andreyev A.Y., Kushnareva Y.E., Starkov A.A., Mitochondrial metabolism of reactive oxygen species, *Biochemistry*, 70 (2005) 200-214.
- [32] Vermes I., Haanen C., Steffens-Nakken H., Reutelingsperger C., A novel assay for apoptosis Flow cytometric detection of phosphatidylserine early apoptotic cells using fluorescein labelled expression on Annexin V. *Journal of Immunological Methods*, 184 (1995) 39-51
- [33] Dasari M., Acharya A.P., Kim D., Lee S., Lee S., Rhea J., Molinaro R., Murthy N., H-gemcitabine: A new gemcitabine prodrug for treating cancer, *Bioconjugate Chem.*, 24 (2013) 4-8.